NOTES AND CORRESPONDENCE

On the Existence of Water Turbulence Induced by Nonbreaking Surface Waves

ALEXANDER V. BABANIN

Swinburne University of Technology, Melbourne, Victoria, Australia

BRIAN K. HAUS

Division of Applied Marine Physics, Rosenstiel School of Marine and Atmospheric Science, University of Miami, Miami, Florida

(Manuscript received 18 December 2008, in final form 23 April 2009)

ABSTRACT

This paper is dedicated to wave-induced turbulence unrelated to wave breaking. The existence of such turbulence has been foreshadowed in a number of experimental, theoretical, and numerical studies. The current study presents direct measurements of this turbulence. The laboratory experiment was conducted by means of particle image velocimetry, which allowed estimates of wavenumber velocity spectra beneath monochromatic nonbreaking unforced waves. Observed spectra intermittently exhibited the Kolmogorov interval associated with the presence of isotropic turbulence. The magnitudes of the energy dissipation rates due to this turbulence in the particular case of 1.5-Hz deep-water waves were quantified as a function of the surface wave amplitude. The presence of such turbulence, previously not accounted for, can affect the physics of the wave energy dissipation, the subsurface boundary layer, and the ocean mixing in a significant way.

1. Introduction

Turbulence can be generated by a sheared fluid motion if a certain inertia-to-viscosity ratio limit is overcome (e.g., Reynolds 1883). Although this should be true in a general case, the motion due to surface water waves is generally regarded to be irrotational (e.g., Young 1999) and thus does not produce shear stresses and turbulence directly. The conjecture of irrotationality in such theories is a consequence of the initial assumption that the waves are free; that is, the waves have no viscosity and surface tension and therefore cannot cause shear stresses (e.g., Komen et al. 1994). Water viscosity, albeit small and negligible from the point of view of many applications, however, is not zero, and the existence of the wave-induced turbulence has been suggested (Babanin 2006). Here we show that such turbulence does exist. In a laboratory experiment, wavenumber velocity spectra beneath surface waves of different steepnesses, in absence of wave breaking, exhibited the Kolmogorov interval associated with the presence of isotropic turbulence. Furthermore, magnitudes of the energy dissipation rates due to this turbulence in the particular case of 1.5-Hz deep-water waves were quantified as a function of the surface wave amplitude. The presence of such turbulence, previously not accounted for, can affect the physics of the wave energy dissipation, the subsurface boundary layer, and the ocean mixing in a significant way.

The turbulence injected by breaking waves is commonly perceived as one of the main means to transfer wind momentum into subsurface waters and has been broadly implemented in ocean circulation and ocean mixing models (e.g., Craig 2005). In contrast, the notion of a nonbreaking wave-induced turbulence is a new concept, although it has been foreshadowed in a number of experimental (Yefimov and Khristoforov 1971; Cavaleri and Zecchetto 1987; Gemmrich and Farmer 2004; Babanin et al. 2005; Gemmrich 2009, manuscript submitted to *J. Phys. Oceanogr.*), theoretical (Thais and Magnaudet 1996; Phillips 2001; Ardhuin and Jenkins

Corresponding author address: Alexander Babanin, Swinburne University of Technology, P.O. Box 218, Hawthorn, Melbourne, VIC 3122, Australia.
E-mail: ababanin@swin.edu.au

DOI: 10.1175/2009JPO4202.1

2006), and numerical studies (Pleskachevsky et al. 2001, 2005; Qiao et al. 2004, 2008; Gayer et al. 2006).

The field experimental studies produce direct and convincing evidence in favor of such turbulence. Yefimov and Khristoforov (1971) provide detailed and quantified data and parameterizations of wave-induced turbulence. Although they did not explicitly account for wave breaking, possible rates of breaking in their experiments were found to be negligible (Babanin 2006). The rest of the mentioned studies explicitly state that wave-related turbulence was observed in absence of wave breaking. In Babanin et al. (2005), in the second set of Cavaleri and Zecchetto (1987) observations, and in Gemmrich (2009, manuscript submitted to *J. Phys. Oceanogr.*) consistent rates of turbulent energy dissipation were observed in the definite absence of wave breaking.

The numerical studies mentioned here provide indirect support for the concept of wave-induced turbulence, as they do not simulate the Navier–Stokes equation. Rather, these works demonstrate that, unless such turbulence exists and is accounted for, it is not possible to explain observed physics both in the deep ocean and in the finite-depth coastal areas. Pleskachevsky et al. (2001, 2005) and Gayer et al. (2006) concluded that, unless they introduce wave-induced turbulent stresses, they cannot explain observed profiles of the suspended sediment at the North Sea shelf and even the very fact of suspension of the previously settled sediments. Qiao et al. (2004, 2008) introduced nonbreaking wave-induced stresses in ocean circulation models coupled with surface waves and achieved dramatic improvements in predictions of the upper-ocean thermal structure and mixed layer depth compared to the traditional mixing schemes.

The physical concept of the turbulence induced directly by nonbreaking waves was originally suggested as a hypothesis of wave amplitude–based Reynolds number

$$\mathrm{Re} = \frac{a^2\omega}{\nu}, \tag{1}$$

which is meant to indicate a transition from laminarity to turbulence for the wave orbital motion (Babanin 2006). Here, a is the wave amplitude (radius of the wave orbit) at the surface, ω is the angular frequency, and ν is the kinematic water viscosity. Estimates of the critical wave Reynolds number provided an approximate value of $\mathrm{Re}_{\mathrm{cr}} = 3000$, and various comparisons were conducted to verify this threshold. The comparisons relied on the ability of the turbulence, generated by wind waves, to mix the upper ocean, and although very supportive, they were still indirect. This article is dedicated to direct measurements of the turbulence induced by surface waves in absence of breaking and wind forcing.

2. Experiment and results

The measurements were conducted in the Air–Sea Interaction Saltwater Tank (ASIST) of the University of Miami. The tank is of stainless steel and acrylic construction with a working section of 15 m $\times$ 1 m $\times$ 1 m. It has a fully programmable wavemaker, able to produce waves with a predefined spectral form, including monochromatic waves. These waves are dissipated at the opposite end of the facility by a minimum-reflection beach.

In the present experiment, to avoid any ambiguity due to wind-caused shear stresses and spectral wave superpositions, a simple setup was realized. Unforced (no wind) mechanically generated monochromatic deep-water two-dimensional wave trains of 1.5 Hz were generated. Particle image velocimetry (PIV) measurements were conducted at 5.1 m from the wavemaker in the center of the tank, directly under the troughs of the deepest waves—that is, always at the same distance from the still surface level of 38.8 cm. The distance of 5.1 m has been shown to be sufficiently far away from the paddle for the wave shape to be well established but shorter than required for intensive modulational instability to develop (Babanin et al. 2007). Measurements were made after the first few waves passed the measurement region but before there could be any reflections off the dissipative beach, which was 9.2 m from the measurement region. The tank has a smooth acrylic bottom and sidewalls that lead to a very thin wave boundary layer ($<$0.005 m). Observations above the bed and near the sidewalls under the wave conditions of interest revealed no upward/outward eddy propagation above the bottom/side boundary layers. Possible contaminations by wave-induced secondary circulations (e.g., Groeneweg and Battjes 2003) were also investigated. The PIV system was positioned to observe the along-tank and cross-tank velocities in a horizontal plane at a level just below the lowest wave troughs (38.8 cm). Measurements of the cross-tank mean flow for the 1.5-Hz waves studied showed that it was very small ($<$2.5 mm s^{-1}) and spatially incoherent.

The PIV system employed here operated at a sampling frequency of 15 Hz. It was a double-pulsed system and the time between the image pairs ranged from 3 to 4 ms, depending on the wave amplitude. The tank was seeded with 50-μm polyamide seeding particle (PSP) beads with a specific gravity of 1.06. A 1-megapixel camera was positioned to look from the side of the tank. The laser was projected from the bottom to provide an

illuminated plane in the along-tank and vertical dimensions at the cross-tank center. The image size was 17 cm (1600 pixels) along tank by 12 cm (1186 pixels) in the vertical for the first series of measurements. In the second set of measurements, the camera was set farther back and the image size/pixel resolution was correspondingly larger. Velocities were computed using an adaptive correlation technique, in which the initial interrogation area was 256 pixels × 256 pixels and in three successive refinement steps, the final horizontal resolution was 1.2 mm. Based on the image pixel size and elapsed time between images, the uncertainty of each velocity observation (Hyun et al. 2003) was ± 0.03 m s^{-1}.

Fifteeen wave periods were recorded for each of the wave trains whose wave amplitudes a ranged from 6 through 32.5 mm (at this amplitude, waves started to break at and before the measurement point; therefore, this measurement was not taken into consideration here). Wave amplitudes were recorded at the measurement location using a digital laser elevation gauge (LEG). An argon-ion (488-nm wavelength, 150 MW) air-cooled laser provided a vertical beam. The intersection of this beam with the surface was detected by a digital line-scan camera at a rate of 100 Hz.

PIV measurements provided spatial distributions of the u (horizontal, parallel to the axis of the tank) and w (vertical) components of the two-dimensional velocity and thus avoided the usual problem of converting the frequency (ω) velocity spectra into wavenumber (k) spectra $P(k)$ in absence of steady advective velocity (Lumley and Terray 1983, Agrawal et al. 1992). If isotropic turbulence is generated, the velocity spectra are expected to exhibit a $k^{-5/3}$ Kolmogorov interval at small scales (high wavenumbers) $k \gg k_s$, where k_s characterizes the source of energy in the dynamic system (e.g., Monin and Yaglom 1971). In our case of the monochromatic wave, $k_s \cong k_{1.5\text{Hz}} = 9.82$ rad m^{-1}; therefore, the wavenumber scales of $k = 20$–2600 rad m^{-1} resolved by the PIV frame provided a sufficiently broad band.

The wave Reynolds numbers (1) for 1.5-Hz waves of surface amplitudes $a = 6$–25.5 mm and the water of 20°C ranged from 330 to 5900 and therefore the transition to turbulence could be expected. The probability of this transition depends strongly on distance z from the surface because the Reynolds number was argued to decay very rapidly as a function of z: Re $\sim \exp(-2kz)$ (Babanin 2006). Measurements directly at the surface, however, were not possible because to obtain the wavenumber spectrum, the entire horizontal layer of measured velocities has to be in the water. For consistency of comparisons, the layer at 30 mm from the still surface was chosen as a compromise, which was close enough to the surface but below the wave troughs for all recorded nonbreaking waves.

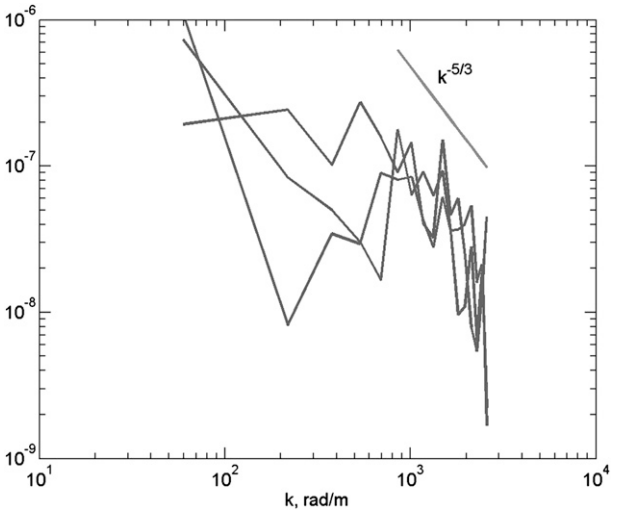

FIG. 1. Velocity spectra exhibiting Kolmogorov interval are shown as solid lines. The $k^{-5/3}$ slope is also shown.

It was expected that the turbulence, subjected to periodic forcing, will exhibit complex and modulated behavior (e.g., Bos et al. 2007). Close to the critical Reynolds number, the turbulence observed was also highly intermittent in both the space and time domains. At the surface wave amplitude of $a = 22.5$ mm at each of the 10 recorded phases of the wave period, the Kolmogorov interval in the velocity spectra appeared from 0 to 3 times over a duration of 15 periods. Most frequently, it was observed at the rear face of the wave profile, close to the instant of zero down crossing, and therefore this phase of the wave was chosen for further analysis.

Examples of the wavenumber spectra recorded during the down crossing, with the turbulence, are demonstrated in Fig. 1. Here, a few P_u spectra exhibiting Kolomogorov interval are shown. The spectra were obtained as Fourier transform of the velocity space series across the 30-mm layer, with averaging over four wavenumbers. Because the size of the image is less than the wavelength, the monochromatic orbital motion peak cannot be seen in the spectrum. The spectra are distinctly different and show clear Kolmogorov subintervals at $k > 800$ rad m^{-1} as should be expected for small turbulence scales far away from the energy source. The Kolmogorov-interval slope is indicated with a straight line.

The level of the Kolmogorov interval contains information about the volumetric kinetic energy dissipation rate ε (Veron and Melville 1999),

$$P(k) = \frac{18}{55}\left(\frac{8\varepsilon}{9\alpha}\right)^{2/3} k^{-5/3}, \qquad (2)$$

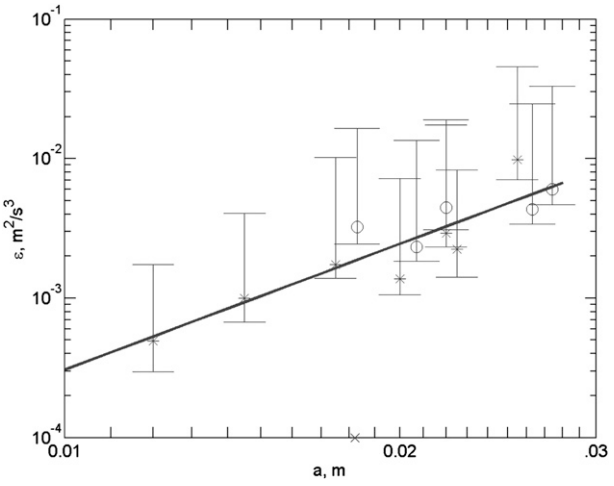

FIG. 2. Dependence of kinetic energy dissipation rate ε vs wave amplitude a. Dependence (3) is shown with solid line. Data points designated with asterisks and circles were obtained in two separate experiments in the same facility. The $\times$ at the bottom axis indicates the value of a, which corresponds to $\mathrm{Re}_{cr} = 3000$. The vertical bars show the standard deviations.

where $\alpha \approx 0.4$ is the Heisenberg constant. Using (2) to define ε, a dependence on the wave amplitude was observed (Fig. 2). Given the large confidence intervals of the individual estimates and the highly intermittent behavior of the observed turbulence, the experiment was repeated to verify the consistency of the result. Data points denoted with circles were obtained, for the same experimental setup, a year later than the asterisk data points.

Direct fit (solid line) provides the dependence

$$\varepsilon = 300a^p. \tag{3}$$

The values of ε and a in this formula are dimensional (see Fig. 2). Because of the scatter, the intercept (coefficient) of this dependence is statistically uncertain; however, for the exponent p in (3), the 95% confidence limit places it between 2 and 4: $p = 3.0 \pm 1.0$. This is close to the expectation (Babanin 2006) that, because the force due to the turbulent stresses is proportional to a^2, the energy dissipation rate should be $\varepsilon \sim a^3$.

3. Discussion

The waves observed were unforced (no wind), mechanically generated, deep-water, two-dimensional wave trains; thus, sources of the shear production were carefully eliminated. Measurements were conducted at the center of the tank, far away from the bottom and sidewall boundary layers, whose effects were thoroughly controlled. The wave trains were monochromatic—no microscale waves and microscale breaking were present. Therefore, the turbulence observed must have been directly generated by the waves themselves. It should also be pointed out that such turbulence production cannot be attributed to Ardhuin and Jenkins (2006) or to similar mechanisms of wave–current–turbulence interactions. Such mechanisms are capable of explaining the transfer of energy from mean orbital motion to the turbulence but only provided that background turbulence already exists. In our case, there was no background turbulence.

It should be emphasized again that the ε estimates obtained are not sustained dissipation rates; they are instantaneous values incurred intermittently at the rearface phase of the wave below the level of the wave trough. Such intermittent turbulence does not reveal a threshold value of wave amplitude, below which it does not occur (i.e., the critical Reynolds number), and the data fit shows the correlation of 89% for the dependence that goes through zero. The value of $a = 0.0182$ m, which corresponds to the critical wave Reynolds number $\mathrm{Re}_{cr} = 3000$ for the 1.5-Hz wave, is marked in Fig. 2 with the "$\times$" at the bottom axis. The lowest wave amplitude, at which the turbulence was still observed (i.e., $a = 0.012$ m) corresponds to $\mathrm{Re} = 1300$. If approximately scaled to the free surface $z = 0$ by assuming $\exp(-kz)$ attenuation of the wave amplitude, the lowest turbulence-producing Reynolds number would be $\mathrm{Re} = 2300$. This is close to the lower-margin estimate of the critical Reynolds number of Babanin (2006). Such scaling, however, is speculative for the measurements just below troughs of the steep waves. Therefore, for the reference estimates, we chose to show the fit going through the origin rather than trying to produce a dependence based on an imposed threshold value for the amplitude.

The levels of the turbulent rates of $\varepsilon \sim 10^{-3}\ \mathrm{m^2\ s^{-3}}$ are quite high and comparable with dissipation rates measured in presence of wave breaking (Agrawal et al. 1992; Young and Babanin 2006). Thus, locally, the wave-induced turbulence can be quite intensive, but its average rates have to be scaled down over the wave period and also due to the intermittency of the observed turbulence, as described above. It is also worth mentioning that in a recent study of turbulence and energy dissipation associated with wave breaking (Gemmrich 2009, manuscript submitted to *J. Phys. Oceanogr.*), it was found that in absence of wave breaking, the turbulent dissipation persists with energy dissipation levels of $\varepsilon \sim 5 \times 10^{-3}\ \mathrm{m^2\ s^{-3}}$. Such levels are in close agreement with the wave-breaking onset levels measured in this study (Fig. 2). Experimental approximation (3) is also consistent with $\varepsilon \sim a^3$ dependence implied by Qiao et al. (2004, 2008), who introduced additional wave-induced turbulent mixing in ocean circulation models. The very

significant advances in performance of such models can be interpreted as an indirect support of the experimental results and dependence (3) presented here.

Although generalizing the results obtained in a particular case of short and steep laboratory waves is not feasible, this may still indicate a significance of the nonbreaking wave-induced turbulence. When comparing breaking and nonbreaking rates directly, our measurements revealed close values: The instantaneous dissipation rates of the $a = 32.5$ mm 1.5-Hz waves at the rear face, where the nonbreaking turbulence was found in this study, and at the front face, where the breaking-in-progress turbulence develops, show magnitudes of $\varepsilon \approx 22.5 \times 10^{-3}$ m^2 s^{-3} and $\varepsilon \approx 14.6 \times 10^{-3}$ m^2 s^{-3}, respectively.

Acknowledgments. The authors gratefully acknowledge the assistance of Ivan Savelyev with measurements and the transfer of the data. BKH was supported by NSF OCE Grant 0526291. Alex Babanin conducted this research with the support of an RDS grant from the Swinburne University of Technology.

REFERENCES

Agrawal, Y. C., E. C. Terray, M. A. Donelan, P. A. Hwang, A. J. Williams III, W. M. Drennan, K. K. Kahma, and S. A. Kitaigorodskii, 1992: Enhanced dissipation of kinetic energy beneath surface waves. *Nature,* **359,** 219–220.

Ardhuin, F., and A. D. Jenkins, 2006: On the interaction of surface waves and upper ocean turbulence. *J. Phys. Oceanogr.,* **36,** 551–557.

Babanin, A. V., 2006: On a wave-induced turbulence and a wave-mixed upper ocean layer. *Geophys. Res. Lett.,* **33,** L20605, doi:10.1029/2006GL027308.

——, I. R. Young, and H. Mirfenderesk, 2005: Field and laboratory measurements of wave-bottom interaction. *Proc. 17th Australasian Coastal and Ocean Engineering Conf. and the 10th Australasian Port and Harbour Conf.,* Adelaide, South Australia, Engineers Australia, 293–298.

——, D. Chalikov, I. R. Young, and I. Savelyev, 2007: Predicting the breaking onset of surface water waves. *Geophys. Res. Lett.,* **34,** L07605, doi:10.1029/2006GL029135.

Bos, W. J. T., T. T. Clark, and R. Rubinstein, 2007: Small scale response and modeling of periodically forced turbulence. *Phys. Fluids,* **19,** Abstract 055107, doi:10.1063/1.2728939.

Cavaleri, L., and S. Zecchetto, 1987: Reynolds stresses under wind waves. *J. Geophys. Res.,* **92C,** 3894–3904.

Craig, P. D., 2005: Modeling turbulence generation by breaking waves. *Marine Turbulence: Theories, Observations and Models,* H. Baumert, J. Simpson, and J. Sündermann, Eds., Cambridge University Press, 273–276.

Gayer, G., S. Dick, A. Pleskachevsky, and W. Rosenthal, 2006: Numerical modeling of suspended matter transport in the North Sea. *Ocean Dyn.,* **56,** 62–77.

Gemmrich, J. R., and D. M. Farmer, 2004: Near-surface turbulence in the presence of breaking waves. *J. Phys. Oceanogr.,* **34,** 1067–1086.

Groeneweg, J., and J. A. Battjes, 2003: Three-dimensional wave effects on a steady current. *J. Fluid Mech.,* **478,** 325–343.

Hyun, B. S., R. Balachandar, K. Yu, and V. C. Patel, 2003: Assessment of PIV to measure mean velocity and turbulence in open-channel flow. *Exp. Fluids,* **35,** 262–267, doi:10.1007/s00348-003-0652-7.

Komen, G. I., L. Cavaleri, M. Donelan, K. Hasselmann, S. Hasselmann, and P. A. E. M. Janssen, 1994: *Dynamics and Modelling of Ocean Waves*. Cambridge University Press, 554 pp.

Lumley, J. L., and E. A. Terray, 1983: Frequency spectra of frozen turbulence in a random wave field. *J. Phys. Oceanogr.,* **13,** 2000–2007.

Monin, A. S., and A. M. Yaglom, 1971: *Mechanics of Turbulence*. Vol. 1, *Statistical Fluid Mechanics,* MIT Press, 769 pp.

Phillips, W. R. C., 2001: On the generalized Stokes drift and pseudomomentum in a spectrum of rotational waves. *J. Fluid Mech.,* **430,** 209–220.

Pleskachevsky, A., J. Hosrstman, and W. Rosenthal, 2001: Modeling of sediment transport in synergy with ocean color data. *Proc. Fourth Berlin Workshop on Ocean Remote Sensing,* Berlin, Germany, 177–182.

——, G. Gayer, J. Hosrstman, and W. Rosenthal, 2005: Synergy of satellite remote sensing and numerical modeling for monitoring of suspended particulate matter. *Ocean Dyn.,* **55,** 2–9.

Qiao, F., Y. Yuan, Y. Yang, Q. Zheng, C. Xia, and J. Ma, 2004: Wave-induced mixing in the upper ocean: Distribution and application to a global ocean circulation model. *Geophys. Res. Lett.,* **31,** L11303, doi:10.1029/2004GL019824.

——, Y. Yang, C. Xia, and Y. Yuan, 2008: The role of surface waves in the ocean mixed layer. *Acta Oceanol. Sin.,* **27,** 30–37.

Reynolds, O., 1883: An experimental investigation of the circumstances which determine whether the motion of water shall be direct or sinuous, and of the law of resistance in parallel channels. *Philos. Trans. Roy. Soc. London,* **174,** 935–982.

Thais, L., and J. Magnaudet, 1996: Turbulent structure beneath surface gravity waves sheared by the wind. *J. Fluid Mech.,* **328,** 313–344.

Veron, F., and W. K. Melville, 1999: Pulse-to-pulse coherent Doppler measurements of waves and turbulence. *J. Atmos. Oceanic Technol.,* **16,** 1580–1597.

Yefimov, V. V., and G. N. Khristoforov, 1971: Spectra and statistical relations between the velocity fluctuations in the upper layer of the sea and surface waves. *Izv. Akad. Nauk SSSR, Fiz. Atmos. Okeana,* **7,** 1290–1310.

Young, I. R., 1999: *Wind Generated Ocean Waves*. Ocean Engineering Series, Vol. 2, Elsevier, 288 pp.

——, and A. V. Babanin, 2006: Spectral distribution of energy dissipation of wind-generated waves due to dominant wave breaking. *J. Phys. Oceanogr.,* **36,** 376–394.